

RF CHARACTERISATION OF NEW COATINGS FOR FUTURE CIRCULAR COLLIDER BEAM SCREENS*

P. Krkotic^{1†}, F. Perez, M. Pont, N. Tagdulang¹, ALBA Synchrotron, Cerdanyola del Valles, Spain
S. Calatroni, CERN, Geneva, Switzerland

X. Granados, J. Gutierrez, T. Puig, A. Romanov, G. Telles, ICMAB, Campus UAB, Bellaterra, Spain

A. N. Hannah, O. B. Malyshev, R. Valizadeh, STFC Daresbury Laboratory, Warrington, UK

D. Whitehead, The University of Manchester, Laser Processing Research Centre, Manchester, UK

J. M. O'Callaghan, Universitat Politecnica de Catalunya CommSensLab, Barcelona, Spain

¹also at Universitat Politecnica de Catalunya - CommSensLab, Barcelona, Spain

Abstract

For the future high energy colliders being under the design at this moment, the choice of a low surface impedance beam screen coating material has become of fundamental importance to ensure sufficiently low beam impedance and consequently guaranteed stable operation at high currents. We have studied the use of high-temperature superconducting coated conductors as possible coating materials for the beam screen of the FCC-hh. In addition, amorphous carbon coating and laser-based surface treatment techniques are effective surface treatments to lower the secondary electron yield and minimise the electron cloud build-up. We have developed and adapted different experimental setups based on resonating structures at frequencies below 10 GHz to study the response of these coatings and their modified surfaces under the influence of RF fields and DC magnetic fields up to 9 T. Taking the FCC-hh as a reference, we will show that the surface resistance for REBCO-CCs is much lower than that of Cu. Further we show that the additional surface modifications can be optimised to minimise their impact on the surface impedance. Results from selected coatings will be presented.

INTRODUCTION

Design studies for future high energy colliders require an active R&D to cope with their demanding technological challenges. This includes higher energies, higher magnetic fields, enlarged accelerator sizes, and a significant increase of synchrotron radiation for circular colliders. For beam screens of high-intensity colliders with positively charged particles, new coatings have to be developed to reduce the surface impedance while simultaneously maintain the secondary electron yield (SEY) low enough to keep e-cloud build-up to a minimum. These new coatings require accurate

characterisation of their electrical properties at microwave frequencies. In this work, we present a resonator capable of performing such tests at conditions (temperatures and DC magnetic fields) similar to those foreseen in the Future Circular Collider (FCC-hh).

MEASUREMENT METHODOLOGY

The measurement method selected for these experiments is based on a Hakki-Coleman dielectric resonator (DR) [1]. Our design (Fig. 1) has been fitted to perform measurements at low temperature under DC magnetic fields and adapted to the size of the samples available. It consists of a cylindrical metallic cavity (radius 5.5 mm, height 3 mm) loaded with a c-oriented, high-permittivity ($\epsilon_r(50K) \approx 110$), and low-loss ($\tan(\delta)(50K) < 10^{-5}$) rutile (TiO_2 , radius 2 mm), shielded axially by a pair of samples to be analysed. The structure sustains a TE_{011} mode [2, 3] in which the induced RF currents on the samples are azimuthal. The absence of radial currents makes the resonator parameters sensitive to the properties of the materials being tested though insensitive to the electrical contact between the samples under test and the lateral walls. This technique has proven capable of measuring surface resistances (R_S) over four orders of magnitude with high reproducibility [4–8].

The measurable resonator parameters Q_0 , and f_0 are related to the surface impedance $Z_s = R_s + iX_s$ through [9, 10]:

$$\frac{1}{Q_0} = \sum_{i=1}^3 \frac{R_{S_i}}{G_i} + p \cdot \tan(\delta), \quad (1)$$

$$-2 \frac{f_0 - f_{0,\text{ref}}}{f_{0,\text{ref}}} = \sum_{i=1}^3 \frac{\Delta X_{S_i}}{G_i} + p \frac{\epsilon_r - \epsilon_{r,\text{ref}}}{\epsilon_{r,\text{ref}}}. \quad (2)$$

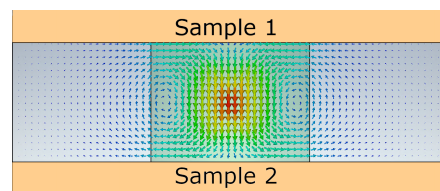


Figure 1: Magnetic field distribution of the TE_{011} mode calculated with CST in the dielectric resonator. Samples are 12 mm \times 12 mm in size.

* Work supported by CERN under Grants FCC-GOV-CC-0210 (KE4945/ATS), FCC-GOV-CC-0209 (KE4946/ATS) and FCC-GOV-CC-0208 (KE4947/ATS). ICMAB funding through RTI2018-095853-B-C21 SuMaTe from MICINN and co-financing by the European Regional Development Fund, 2017-SGR 1519 from Generalitat de Catalunya, and COST Action NANOCO-HYBRI (CA16218) from EU, the Center of Excellence award Severo Ochoa CEX2019-000917-S. UPC funding through the Unit of Excellence Maria de Maetzu MDM2016-0600. N. Tagdulang and A. Romanov acknowledge MSCA-COFUND-2016-754397 for the PhD grant.

[†] pkrkotic@cells.es, patrickkrkotic@outlook.de

Here, Q_0, f_0 , and $f_{0,ref}$ are the unloaded quality factor, resonance frequency and reference resonance frequency, respectively; $R_{S_i}, \Delta X_{S_i}, p, \tan \delta$ and G_i are the surface resistance, incremental change of surface reactance with respect to a reference value, dielectric filling factor, dielectric loss tangent and the geometrical factor of the i -th conductive surface of the cavity, respectively. Note that the dielectric filling factor p and the geometrical factors G_i depend entirely on the distribution of electromagnetic fields in the cavity and are independent of material properties [9].

To accurately post-process the acquired measurement data, the unloaded quality factor and resonant frequency data is obtained from measurements of reflection and transmission coefficients (S-parameters). The evaluation of the S-parameters is done by using an algorithm implemented into an open-source, web-executable application [12] based on Moore-Penrose inverse routines which includes an adaptive outlier removal procedure that discards distorted measurement points [13].

Since this experimental technique is not capable of measuring the absolute values of X_S , the reference values $f_{0,ref}, X_{S,ref}$ are required to calculate its incremental changes with respect to its values at a given reference, e.g. 0 T. Theoretically, we can determine the absolute value of the surface reactance for a superconductor through [11]:

$$X_{S,ref} = 2\pi f_{0,ref} \lambda_L \mu_0, \quad (3)$$

where λ_L is the London penetration depth, and μ_0 is the vacuum permeability. In this way, we can obtain absolute values for the surface reactance for superconducting samples. In the case of normal conducting metals, in the normal skin effect regime, $R_S = X_S$ commonly applies.

SAMPLE CHARACTERISATION

In a round pipe with a uniform coating in the ultra-relativistic limit, the longitudinal and transverse resistive wall (RW) impedance Z_{RW} depends linearly on the surface impedance Z_S of the coating material [14]. Hence, lowering the surface impedance has a direct impact on the Z_{RW} experienced by the beam. Additionally, the coating should have a low secondary electron yield (SEY) to keep e-cloud build-up to a minimum. Different surface treatments such as amorphous carbon (a-C) coating -baseline surface treatment for the HL-LHC [15]- and surface topography changes through laser ablation of metals [16, 17] have been proposed and tested. Surface modification of the coating material increases normally its surface impedance. Therefore, a compromise between SEY and surface impedance has to be established.

Metal Coatings

Laser ablation surface engineering (LASE) and laser-engineered surface structures (LESS) have shown its potential [8, 15] to reduce the SEY of metallic coatings. We have performed direct R_S measurements on samples with different LASE treatments. Table 1 indicates the LASE

treatment parameters used on the samples of this study. The treated copper (Cu) materials are divided into two sets with three sample pairs, each using the same laser but a different repetition rate, ergo different energy per pulse deposited. Figure 2 shows the surface resistance of the LASE treated samples compared to FCC-hh Cu sputtered on stainless steel as a function of temperature. Despite the evident difference in the magnitude of R_S between the two sets shown in the figure, both sets follow the same pattern. The smaller the pitch, the higher the R_S . This can be understood if we consider that the closer the scanning lines, the larger the ratio between treated and untreated material.

There is a relatively low increase of R_S compared to FCC-hh Cu of about 15% for the samples treated with a repetition rate of 600 kHz. These findings are complementary to those of a previous study in [8]. For samples treated with 600 kHz repetition rate, the measured surface resistance is comparable to the one reported in [8], therefore we can predict similar behaviour on the SEY around $\delta_{SEY} \approx 2.2$. For the samples treated at a lower repetition rate 30 kHz, we can predict SEY values $\delta_{SEY} \approx 1$. In this case, the low SEY comes at the expenses of a surface resistance about 60% above that of FCC-hh Cu.

Table 1: LASE Treatment Parameters

Repetition Rate, Energy Per Pulse	Pitch		
Set 1 - 600 kHz, 0.05 μ J	100 μ m	10 μ m	2 μ m
Set 2 - 30 kHz, 1 mJ	100 μ m	10 μ m	2 μ m

The laser (1063 nm and 30 W average power) has a pulse duration of 150 ps to 2 ns at the two given repetition rates, respectively.

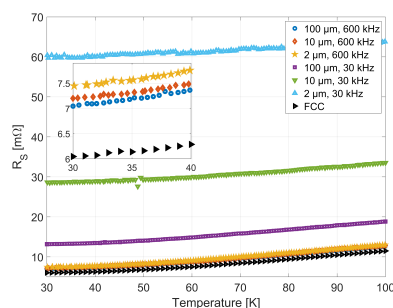


Figure 2: Surface resistance of several laser treated samples versus temperature. The first value in the legend refers to the pitch whereas the second value states the repetition rate of the laser.

High-Temperature Superconducting Coated Conductors

An alternative to reduce the surface resistance well below that of Cu is the use of $REBa_2Cu_3O_{7-x}$ coated conductors (REBCO CCs, RE = Y, Gd, Eu) as coating materials. These

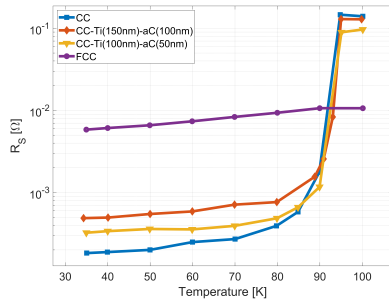


Figure 3: Surface resistance for a coated conductor (CC) with and without sputtered titanium (Ti) and amorphous carbon (a-C) of different thickness as a function of temperature including FCC copper (FCC).

High-Temperature superconductors (HTS) have transition temperatures around 90 K and have demonstrated surface resistances well below that of Cu under a 9 T magnetic field at about 8 GHz [6]. A main disadvantage of REBCO-CCs is the poor secondary electron yield values measured [6]. Nonetheless, an amorphous carbon (a-C) coating has been proposed as a solution for this problem. Due to its low conductivity, very thin a-C top layers should not affect the overall surface resistance. A titanium (Ti) sub-layer has been used during the sputtering process to improve the adhesion of the a-C layer. In [6] we presented that this multi-layer coating on a CC reduces the SEY values from $\delta_{SEY,CC} \approx 3$ to $\delta_{SEY,CC,Ti,a-C} \approx 1.3$. Figure 3 shows the measured R_S values of a REBCO-CC and two such multi-layer samples as a function of temperature. One can clearly see the transition temperature around 92 K. Even though there is a two- to three-fold increase in R_S depending on the total multi-layer thickness, the resulting R_S is still one order of magnitude lower than that of FCC-hh copper in the same conditions.

Figure 4 shows the increments with respect to the reference value measured at 0 T in surface resistance and reactance at 50 K, as a function of a perpendicularly applied DC magnetic field up to 9 T after cooling the samples in zero field. Both quantities rise with increasing magnetic field. However, the absolute change in the surface reactance is much larger than for the surface resistance. Using a London penetration depth $\lambda_L = 157$ nm at 50 K and equation (3) one can calculate the absolute surface reactance at 0 T to be $X_{S,ref} = 9.82$ m Ω . The value of the surface reactance as a function of the magnetic field can be calculated from the values given in Fig. 4.

The R_S of the REBCO-CC multi-layer stays lower than that of FCC-copper up to 9 T at 50 K, while X_S is higher than FCC Cu in these conditions: $Z_S = (1 + i) 6.71$ m Ω for Cu, compared to $Z_S = (0.19 + i9.82)$ m Ω for REBCO-CC.

Note that these are surface impedances at 7.9 GHz, close to the upper end of the expected beam frequency spectrum of the FCC-hh. Extrapolating the data in Fig. 4 with a linear fit up to 16 T, and in addition, assuming a square frequency dependence on R_S and a linear frequency dependence on X_S ,

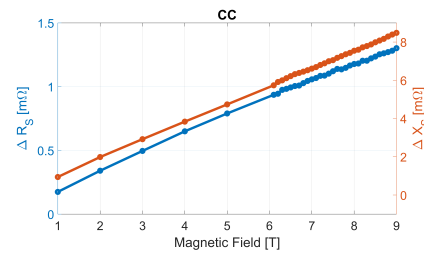


Figure 4: Changes in surface impedance as a function of applied magnetic field at 50 K. In blue the measured changes in the surface resistance and in red the changes in the surface reactance

one can extrapolate further these results to 1 GHz as shown in Table 2. The estimation shows that the surface resistance of REBCO-CC will have values much lower than those of Cu up to 16 T, while the surface reactance will remain lower until a certain crossing point, which is in good agreement with [7]. One has to mention that in this relatively simple approach, we have neglected any residual surface impedance, e.g. due to nano-inclusions in the REBCO-CC, as well as the entrance into the anomalous skin effect regime for copper. Furthermore, one has to explain that while the surface resistance quantifies the power absorbed by the material, the surface reactance characterises the stored electromagnetic energy. Vortex penetration of the magnetic field inside the CC combined with RF currents in the superconducting materials results in a movement of vortices which affect stored and dissipated energy and hence, the material's surface impedance.

Table 2: Extrapolated surface impedance values at 50 K, 16 T and 1 GHz.

Material	CC	FCC Cu
Z_S [m Ω]	0.039 + i 3.12	2.38 + i 2.38

CONCLUSION

We have described the use of dielectric resonators to characterise beam screen coatings by providing results of surface impedance under working conditions that approach those found on high energy colliders. We have also shown results on advanced coatings and surface treatments that reduce the SEY effectively while keeping the surface resistance at high frequencies comparable to or below that of untreated surfaces. Extrapolation of measured results to FCC-hh conditions suggests the advantageous performance of these materials in terms of SEY and beam impedance parameters.

REFERENCES

- [1] B. W. Hakki and P. D. Coleman, "A Dielectric Resonator Method of Measuring Inductive Capacities in the Millimeter Range", *IRE Trans. Microwave Theory Tech.*, vol. 8, no. 4, pp. 402-410, Jul. 1960. doi: 10.1109/TMTT.1960.1124749

- [2] Z.-Y. Shen *et al.*, “High- T_c Superconductor-Sapphire Microwave Resonator with Extremely High Q-Values up to 90 K”, *IEEE Trans. Microwave Theory Tech.*, vol. 40, pp. 2424-2431, Dec. 1992. doi:10.1109/22.179912
- [3] J. Mazierska and R. Grabovickic, “Circulating power, RF magnetic field, and RF current density of shielded dielectric resonators for power handling analysis of high-temperature superconducting thin films of arbitrary thickness”, *IEEE Trans. Appl. Supercond.*, vol. 8, pp. 178–187, Dec. 1998. doi:10.1109/77.740683
- [4] P. Krkotić *et al.*, “Small Footprint Evaluation of Metal Coatings for Additive Manufacturing”, in *Proc. 48th European Microwave Conference (EuMC)*, Madrid, Spain, Sep. 2018, pp. 882-885. doi:10.23919/EuMC.2018.8541442
- [5] D. Arcos *et al.*, “Contactless Electrical Resistance of 2D Materials Using a Rutile Resonator”, *Phys. Status Solidi B*, vol. 256, no. 12, p. 1900428, Nov. 2019. doi:10.1002/pssb.201900428
- [6] T. Puig *et al.*, “Coated conductor technology for the beam-screen chamber of future high energy circular colliders”, *Supercond. Sci. Technol.*, vol. 32, p. 094006, Jul. 2019. doi:10.1088/1361-6668/ab2e66
- [7] A. Romanov *et al.*, “High frequency response of thick REBCO coated conductors in the framework of the FCC study”, *Sci. Rep.*, vol. 10, Jul. 2020. doi:10.1038/s41598-020-69004-z
- [8] A. N. Hannah *et al.*, “Characterisation of copper and stainless steel surfaces treated with laser ablation surface engineering”, *Vacuum*, vol. 189, p. 110210, Jul. 2021. doi:10.1016/j.vacuum.2021.110210
- [9] D. Kajfez and P. Guillon, *Dielectric Resonators Antenna Handbook*. USA: Artech House, 1986.
- [10] N. Pompeo *et al.*, “Dielectric Resonators for the Measurements of the Surface Impedance of Superconducting Films”, *Meas. Sci. Rev.*, vol. 14, pp. 164–170. May 2014. doi:10.2478/msr-2014-0022
- [11] M. Hein, *High-Temperature-Superconductor Thin Films at Microwave Frequencies*. Berlin, Germany: Springer-Verlag, 1999.
- [12] ARPE, www.arpe.upc.edu
- [13] P. Krkotić *et al.*, “Algorithm for Resonator Parameter Extraction From Symmetrical and Asymmetrical Transmission Responses”, *IEEE Trans. Microwave Theory Tech.*, recently accepted for publication, 2021. doi:10.1109/TMTT.2021.3081730
- [14] R. Gluckstern, “Analytic methods for calculating coupling impedances”, CERN, Geneva, Switzerland, Rep. CERN-2000-011, 2000.
- [15] S. Calatroni *et al.*, “Cryogenic surface resistance of copper: Investigation of the impact of surface treatments for secondary electron yield reduction”, *Phys. Rev. Accel. Beams.*, vol. 22, p. 063101, Jun. 2019. doi:10.1103/PhysRevAccelBeams.22.063101
- [16] R. Valizadeh *et al.*, “Low secondary electron yield engineered surface for electron cloud mitigation”, *Appl. Phys. Lett.*, vol. 105, p. 231605, Nov. 2014. doi:10.1063/1.4902993
- [17] G. Tang *et al.*, “Nanosecond pulsed laser blackening of copper”, *Appl. Phys. Lett.*, vol. 101, p. 231902, Nov. 2012. doi:10.1063/1.4769215